A Context-Sensitive Technique Robust to Registration Noise for Change Detection in VHR Multispectral Images

Silvia Marchesi, *Student Member, IEEE*, Francesca Bovolo, *Member, IEEE*, and Lorenzo Bruzzone, *Fellow, IEEE*

***Abstract*—This paper presents an automatic context-sensitive technique robust to registration noise (RN) for change detection (CD) in multitemporal very high geometrical resolution (VHR) remote sensing images. Exploiting the properties of RN in VHR images, the proposed technique analyzes the distribution of the spectral change vectors (SCVs) computed according to the change vector analysis (CVA) in a quantized polar domain. The method studies the SCVs falling into each quantization cell at different resolution levels (scales) to automatically identify the effects of RN in the polar domain. This information is jointly exploited with the spatial context information contained in the neighborhood of each pixel for generating the final CD map. The spatial context information is modeled through the definition of adaptive regions homogeneous both in spatial and temporal domain (parcels). Experimental results obtained on real VHR remote sensing multitemporal images confirm the effectiveness of the proposed technique.**

***Index Terms*—Change detection (CD), change vector analysis (CVA), multitemporal images, registration noise (RN), remote sensing, very high resolution (VHR) images.**

I. Introduction

UNSUPERVISED change detection plays an important role in many application domains related to the exploitation of multitemporal images. Depending upon the considered application, the change-detection problem has different properties and peculiarities, and should satisfy specific constraints. In some domains, the priority constraint is related to the need to guarantee a real time detection of changes (e.g., in video surveillance [1]–[4], motion detection [5], [6], etc.). In other applications, the time constraint can be relaxed and the precision of the change-detection result (also at the cost of a high computational complexity) plays the most important role (e.g., remote sensing [7], [8], biomedical applications [9], [10], etc). For some domains, the change-detection problem can require multidimensional (or multichannel) images: this is for instance the case of data simultaneously acquired in different bands of the electromagnetic spectrum (multispectral images) or taken with multimodal acquisition protocols (multimodal images). In this perspective, the change-detection procedure is more complex and should be able to recognize the presence of changes by analyzing multidimensional vectors associated with each pixel of the investigated multitemporal images. Typical applications related to the above-mentioned data are in the remote sensing and the biomedical domains.

In this paper we focus the attention on unsupervised change-detection techniques for multitemporal and multispectral remote sensing images. In greater detail, we consider very high geometrical resolution multispectral images acquired by the last generation of satellite sensors (e.g., Ikonos, QuickBird, EROS, SPOT-5, GeoEye-1, World View-2). These sensors can acquire both multispectral and/or panchromatic images with a geometrical resolution on the ground which varies from few meters to 0.41[m] in the best case (at the time of writing). In the literature, several unsupervised change-detection methods for multidimensional remote sensing images have been proposed [11]–[17]. These techniques have been successfully employed in many different application domains related to land cover monitoring, like analysis of growth of urban areas, cadastral map updating, risk analysis, damage assessment, etc. However, the most of the available methods are optimized for the analysis of images acquired by medium resolution (MR) and high resolution (HR) sensors, and result ineffective when dealing with images showing metric or submetric resolution. Therefore it is necessary to develop novel methodologies capable to exploit the properties of VHR images in detecting changes between multitemporal images.

Change-detection techniques developed in other application domains for the specific analysis of VHR images result ineffective when applied to remote sensing images. The main problems are related to the different conditions in which the remote sensing images can be acquired, and in particular to differences in: 1) sunlight and atmospheric conditions; 2) sensor acquisition geometry [8], [11], [18]; and 3) spectral signatures of vegetation due to seasonal effects. In order to reduce the impact of these conditions on CD maps, preprocessing steps are required as: coregistration, radiometric and geometric corrections, and noise reduction. Among them, coregistration plays a fundamental role and becomes more complex and critical (and therefore intrinsically less accurate), when the geometrical resolution increases. In practice, a perfect alignment between images is impossible as differences in the acquisition view angles and in geometrical distortions cannot be compensated, then causing a significant residual registration noise which sharply impacts on CD [18]–[20].

Manuscript received June 04, 2009; revised January 28, 2010. First published March 08, 2010; current version published June 16, 2010. The associate editor coordinating the review of this manuscript and approving it for publication was Dr. John Kerekes.

The authors are with the Department of Information Engineering and Computer Science, University of Trento, Via Sommarive, 14 I-38123, Trento, Italy (e-mail: silvia.marchesi@disi.unitn.it; francesca.bovolo@disi.unitn.it; lorenzo.bruzzone@ing.unitn.it).

Digital Object Identifier 10.1109/TIP.2010.2045070

Another important problem in change detection on VHR images concerns the modeling of the spatial context information of the scene. Most of the classical change-detection techniques generally assume spatial independence among pixels, which is not reasonable in high geometrical resolution data. In order to better exploit the spatial correlation among neighboring pixels and to get accurate and reliable CD maps (both in regions corresponding to border or geometrical details and in homogeneous areas), it is necessary to integrate the spectral information with the spatial one and to model the multiscale properties of the scene. In the literature only few techniques capable to exploit the above-mentioned concepts [21]–[24] are available.

In order to overcome the aforementioned problems, this paper presents an adaptive context-sensitive technique, which: 1) reduces the impact of registration noise in change detection on VHR multispectral images through a multiscale strategy; and 2) considers the spatial dependencies of neighborhood pixels through the definition of multitemporal parcels (i.e., homogeneous region both in space and time domain). The proposed technique is developed in the context of the polar framework for change vector analysis (CVA) introduced in [16] for the analysis of MR and HR multispectral images, and is based upon the analysis of the properties of registration noise presented in [25]. The experiments carried out on multitemporal VHR images confirm the validity of the theoretical analysis and the effectiveness of the proposed technique.

The paper is organized into five sections. The next section recalls the notation and the background on the polar framework proposed in [16], and describes the registration noise properties derived in [25]. Section III illustrates the proposed multiscale and context-based approach for change detection on VHR images. Section IV presents the experimental results obtained on two real multitemporal data sets made up of QuickBird images. Finally, Section V draws the conclusions of this work. Appendix I provides a summary of the notation used in this paper.

II. Notation and Background

In order to develop the proposed change-detection technique robust to registration noise, we take advantage from the theoretical and empirical analysis on the properties of this kind of noise conducted in [25]. In particular, we consider the properties of registration noise derived in this work as a starting point for the development of our approach. Both the analysis on the properties of registration noise and the proposed technique are developed in the context of a theoretical polar framework defined for unsupervised change detection in [16], which is based upon the change vector analysis (CVA) technique. In the following we briefly recall the main concepts of this framework and the main properties of registration noise.

A. Polar Framework for Change Detection

Let us consider two VHR multispectral images $\mathbf{X}_1$ and $\mathbf{X}_2$ (e.g., Ikonos, QuickBird, EROS, SPOT-5, GeoEye-1, World View-2 images) acquired on the same geographical area at different times t_1 and t_2, respectively. Let us assume that these images do not show significant radiometric differences; in particular, let us consider that the spectral channels at the two times have the same mean values (this can be easily obtained with very simple radiometric correction procedures). Let $\Omega = \{\omega_n, \Omega_c\}$ be the set of classes of changed and no-changed pixels to be identified. In greater detail, ω_n represents the class of no-changed pixels, while $\Omega_c = \{\omega_{c_1}, \ldots, \omega_{c_K}\}$ the set of the K possible classes (kinds) of changes occurred in the considered area. For simplicity, the whole analysis on the registration noise properties is carried out considering a 2-D feature space (however it can be generalized to the case of more features, see [16] for details). In this manner it is possible to represent the information in a 2-D domain and to better understand the implications of the analysis. Let $\mathbf{X}_D$ be the multispectral difference image computed according to the CVA technique by subtracting the spectral feature vectors associated with each corresponding spatial position in the two considered images. $\mathbf{X}_D$ is a multidimensional image made up of spectral change vectors (SCVs) defined as

$$\mathbf{X}_D = \mathbf{X}_2 - \mathbf{X}_1. \tag{1}$$

Under the assumption of 2-D feature vectors, the change information contained in the SCVs can be univocally described by the change vector magnitude ρ and direction ϑ defined as

$$\vartheta = \tan^{-1}\left(\frac{X_{1,D}}{X_{2,D}}\right) \text{ and } \rho = \sqrt{(X_{1,D})^2 + (X_{2,D})^2} \tag{2}$$

where $X_{b,D}$ is the random variable representing the bth component (spectral channel) of $\mathbf{X}_D$ ($b = \{1, 2\}$). Finally, let us define the magnitude-direction domain MD (in which all the SCVs of a given scene are included) as

$$MD = \{\rho \in [0, \rho_{\max}] \text{ and } \vartheta \in [0, 2\pi]\} \tag{3}$$

where ρ_{max} is the highest magnitude of SCVs in the considered images.

According to the previous definitions, the change information for a generic pixels in spatial position (i, j) can be represented in the magnitude-direction domain with a vector z_{ij} having components ρ_{ij} and ϑ_{ij} computed according to (2).

From the theoretical analysis reported in [16] and under the above-mentioned assumptions, it is expected that in the polar representation no-changed and changed SCVs result in separated clusters. Unchanged SCVs show a low magnitude and are uniformly distributed with respect to the direction variable. In the polar domain the region associated with them is the *circle of no-changed pixels* C_n, defined as

$$C_n = \{\rho, \vartheta : 0 < \rho \leq T \text{ and } 0 \leq \vartheta < 2\pi\}. \tag{4}$$

This circle is centered at the origin and has a radius equal to the optimal (in the sense of the theoretical Bayesian decision theory) threshold T that separates no-changed from changed pixels. On the opposite, changed SCVs are expected to show a high magnitude. The region associated with them in the polar domain is the *annulus of changed pixels* A_c, which is defined as

$$A_c = \{\rho, \vartheta : T \leq \rho < \rho_{\max} \text{ and } 0 \leq \vartheta < 2\pi\}. \tag{5}$$

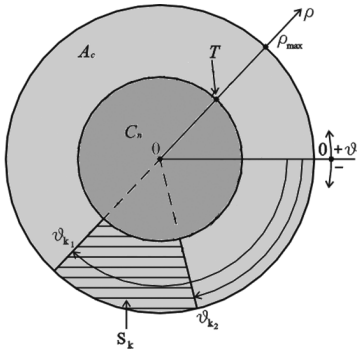

Fig. 1. Representation of the regions of interest in the CVA polar framework.

This annulus has inner radius T and outer radius given by the maximum among all possible magnitudes for the considered pair of images $(\rho_{\max})$. As changed SCVs show preferred directions according to the kind of change occurred on the ground, different kinds of changes can be isolated with a pair of threshold values (ϑ_{k_1} and ϑ_{k_2}) in the direction domain. Each pair of thresholds identifies an *annular sector* S_k *of change* $\omega_{c_k} \in \Omega_c$ in the *annulus of changed pixels* A_c defined as

$$S_k = \{\rho, \vartheta : \rho \geq T \text{ and } \vartheta_{k_1} \leq \vartheta \leq \vartheta_{k_2}, 0 \leq \vartheta_{k_1} < \vartheta_{k_2} \leq 2\pi\}. \quad (6)$$

All the mentioned regions are depicted in Fig. 1. The reader is referred to [16] for further details on both the polar framework and the general properties of SCVs in this kind of representation.

B. Registration Noise Properties

As previously mentioned, residual misregistration affects multitemporal data and represents an important source of noise. In particular, this noise becomes more relevant when dealing with VHR images, as the process of co-registration is more complex and critical. RN is due to the comparison of pixels that do not represent the same area on the ground in images acquired over the same geographical area at different times. In particular, the most critical component of RN is related to the pixels that at the two dates belong to different objects/classes on the ground due to the misalignment between the two images. In fact, these pixels show a behavior similar to the one of real changes, causing misclassification effects in the change-detection process. It follows that it is important to identify these pixels and separate them from pixels associated with real changes in the definition of a change-detection technique robust to registration noise.

In [25], the effects of misregistration have been analyzed in the context of the previous described polar framework when: 1) the misalignment between the images increases, and 2) the resolution (scale) of the images decreases. From this study, four important properties of registration noise in VHR images can be derived for both no-changed and changed pixels.

1) Property 1: Increasing the misalignment between the images, it is possible to observe that RN affects no-changed pixels by: (a) increasing the spread of the cluster in the circle of no-changed pixels C_n with respect to the case of perfectly aligned images; (b) generating clusters of dominant registration noise with properties very similar to clusters of changed pixel in the annulus of changed pixels A_c.

The first effect is related to the non perfect alignment between multitemporal pixels belonging to the same object, while the second one is mainly induced from edge regions and details (high spatial frequencies in the images), which lead to the comparison of pixels belonging to different objects. These pixels result in clusters of registration noise in A_c and involve false alarms in the change-detection map.

2) Property 2: Statistical properties of clusters associated with changed pixels in A_c slowly vary with the amount of misalignment.

This second property results in the conclusion that registration noise does not affect significantly the clusters of changed pixels. This is reasonable because when changes are present the effect of registration noise are often included in the modification of the spectral signature due to the change on the ground.

In this work we are more interested to properties 3 and 4 which are related to the impact of the scale on registration noise properties. To properly illustrate these properties let us consider a pansharpened QuickBird image of 984 × 984 pixels acquired on the city of Trento (Italy) in July 2006 $(\mathbf{X}_1)$.[1] From this image a second image was generated $(\mathbf{X}_2)$ simulating new houses on the rural area. Such changes were introduced in order to be as similar as possible to real changes. In particular, simulated buildings have been added to the scene taking their geometrical structures and spectral signatures from other real buildings present in different portions of the available full scene [25]. This choice allowed us to take into account the image dynamic and also the noise properties. Moreover $\mathbf{X}_1$ and $\mathbf{X}_2$ were relatively shifted for reproducing registration noise effects in a controlled framework. To both images a *Daubechies*-4 stationary wavelet multiscale decomposition [26] was applied in order to obtain a set of multitemporal datasets at different resolution levels (for further details, refer to [25]). Then we applied the CVA to the obtained multiscale and multitemporal images. Misregistration appears in the magnitude image with linear (or non linear) and relatively thin structures having different orientations. Therefore, if we reduce the resolution of images, we implicitly decrease the impact of the registration noise with respect to that on the original scene. The scatterograms in Fig. 2 show the statistical distributions of SCVs obtained according to CVA in the polar domain for the misregistered dataset: (a) at full resolution; and (b) at level 3 of the wavelet decomposition. Comparing the scatterograms it can be observed that reducing the scale, SCVs associated with RN [dashed circles in Fig. 2(a)] tend to disappear collapsing into C_n, while the cluster of pixels associated with true changes (region marked with continuous circles in Fig. 2) reduces its spread, but it is not completely smoothed out. This is confirmed from Fig. 3, which separately reports the behavior of the mean value of the magnitude of SCVs associated with RN (continuous line) and real changes (dashed lines). As can be seen from the diagram, the mean value of the magnitude of SCVs associated with RN decreases faster than the mean value of clusters of changed pixels by reducing the resolution. Therefore, at low resolution levels (where high spatial frequencies are cut off)

[1]For further detail about this image refer to Section IV-A.

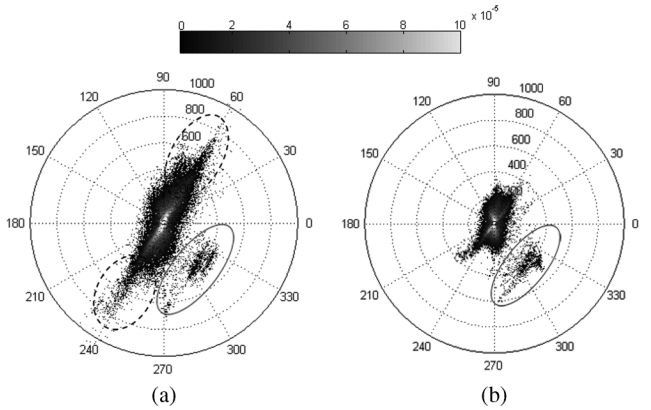

Fig. 2. Scatterograms in the polar coordinate system obtained by applying the CVA technique to the simulated data sets containing changes (a) at full resolution, and (b) at a lower scale. Continuous circle indicates the cluster of true changes, while dashed circles identify regions of registration noise.

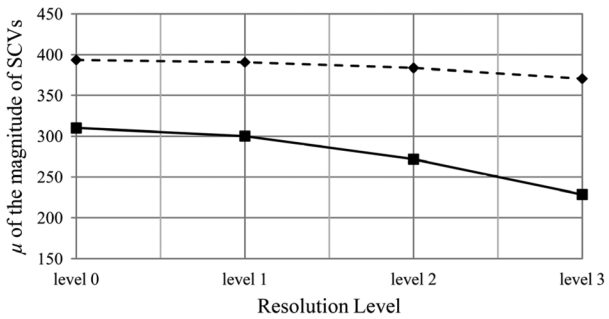

Fig. 3. Behavior of the mean value of the magnitude of SCVs versus the resolution levels (scale) for clusters of change (dashed line) and of registration noise (continuous line).

the impact of the registration noise is lower than at high resolution levels; accordingly, in the *annulus of changed pixels* mainly clusters due to presence of true changes on the ground can be detected. This simple observation on the behavior of SCVs with respect to the scale, and in particular the different behaviors of SCVs of changes and of RN versus scale variations, suggest us important strategies to adopt in the definition of a change-detection technique robust to registration noise. It is important to note that this behavior of cluster associated with true changes holds under the reasonable assumption that they are associated with objects with a non negligible size, compared with the very high geometrical resolution of images.

From the presented analysis and according to [25], two important properties can be derived for what concerns the effects of a scale reduction on the registration noise properties:

3) Property 3: Clusters associated with registration noise in A_c exhibit significant variations of properties versus the scale;

4) Property 4: Clusters of changes exhibit slowly varying statistical properties.

From these two properties it follows that the behaviors of changed and no-changed (i.e., the ones due to RN) SCVs that fall in A_c versus the scale are different: decreasing the scale, sectors of changes, unlike sectors of registration noise, are preserved. This results in an intrinsic robustness of changes to the scale.

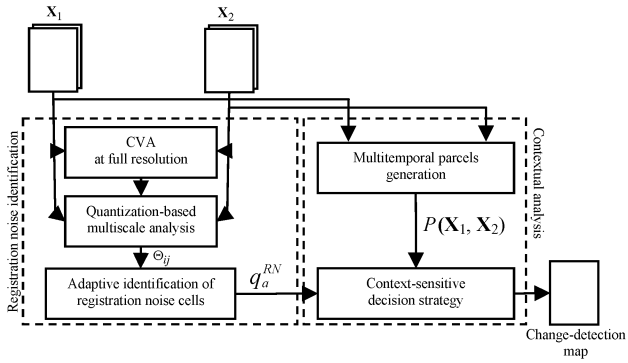

Fig. 4. General architecture of the proposed multiscale and parcel-based change-detection technique.

III. Methodology

The multiscale properties of registration noise briefly recalled in the previous section are at the basis of the development of a change-detection technique based upon the analysis of the behavior of the distribution of SCVs in the polar domain at different scales. As reported in the previous section, we expect that true significant changes are associated with objects with a non negligible size (this assumption is reasonable and realistic when dealing with VHR images), while misregistration appears in the multispectral difference image with relatively thin structures having different orientations. Therefore, by reducing the resolution of images we implicitly decrease the impact of the registration noise with respect to that on the original scene, while the statistical properties of true changes maintain a good stability. In other words, the lower the geometrical resolution is, the lower the probability of identifying clusters associated with registration noise in the *annulus of changed pixels*. This means that at low resolution levels in the *annulus of changed pixels* mainly clusters due to the presence of true changes on the ground can be detected. However, in order to obtain a change-detection map characterized by a good geometrical fidelity, we should work at full resolution. On the basis of these considerations, we propose a change-detection technique that exploits a multiscale decomposition in order to extract information about registration noise, and generates the final change-detection map working at full resolution. In this way we preserve the high geometrical detail content of VHR images. In addition, in order to exploit the specific properties of VHR images, the proposed technique adaptively models also the spatial context information.

The proposed method can be divided into two main phases: 1) registration noise identification; and 2) context-sensitive decision strategy for the generation of the final change-detection map. The main idea of the developed technique is to detect the regions of the polar framework where the registration noise is dominant according to a multiscale strategy, and to consider the spatial-context information through the definition of multitemporal parcels in order to generate the final change-detection map (see Fig. 4). In the following details on the two phases are reported.

A. Registration Noise Identification

The first phase of the proposed technique aims at identifying the regions related to registration noise in the polar domain. To

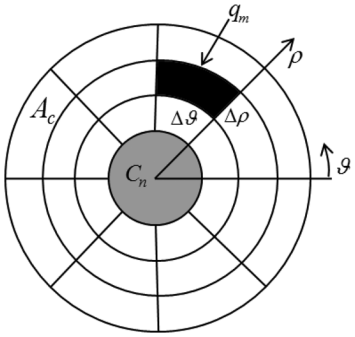

Fig. 5. Quantized magnitude-direction polar domain.

this purpose, we apply an analysis based upon the following three steps: 1) CVA at full resolution (identification at full resolution of regions in the polar domain candidate to include registration noise SCVs, i.e., A_c); 2) quantization-based analysis of the SCV distributions at different resolution levels; and 3) adaptive identification of registration noise cells.

In the first step the CVA technique is applied to the original images $\mathbf{X}_1$ and $\mathbf{X}_2$, and the threshold value T that separates the *circle of no-changed pixels* from the *annulus of changed pixels* is estimated. The value of T can be retrieved either by a manual *trial-and-error* procedure or by one of the automatic thresholding algorithms proposed in the literature [17], [27]. SCVs in C_n are labeled as no-changed SCVs, whereas pixels in A_c should be further analyzed in order to separate SCVs associated with registration noise from pixels of true changes.

To this end, in the second step, A_c is divided into M uniformly distributed quantization cells q_m $(m = 1,\ldots,M)$ $(A_c = \{q_1, q_2, \ldots, q_M\})$ of fixed shape and size. Each cell is characterized by its extension $\Delta\rho$ and $\Delta\vartheta$ in the magnitude and in the direction coordinates, respectively (see Fig. 5). It is worth noting that the choice of the cell size can significantly affect the performance of the quantization-based registration-noise-identification process. The proposed method aims at overcoming this problem by exploiting different cell sizes in the identification of registration noise clusters in A_c (see the third step of the estimation procedure). Once cells have been defined, the two multitemporal images are decomposed according to a multiscale transformation obtaining two sets of images $\mathrm{X}_{MS_t} = \{\mathbf{X}_t^0, \ldots, \mathbf{X}_t^n, \ldots, \mathbf{X}_t^{N-1}\}$, where the subscript $t(t = 1,2)$ denotes the acquisition date, and the superscript n $(n = 0,1,\ldots,N-1)$ indicates the resolution level $(\mathbf{X}_t^0 = \mathbf{X}_t)$. The multiscale decomposition can be carried out by using different algorithms, like gaussian pyramid decomposition, wavelet transform, recursively upsampled bicubic filter, etc. Images in X_{MS_t} show different tradeoffs between registration noise and geometrical detail content. The CVA technique is applied to each corresponding pair $(\mathbf{X}_1^n, \mathbf{X}_2^n)$, $n = 1,2,\ldots,N-1$, of low resolution images in X_{MS_1} and X_{MS_2}. Then the distribution of SCVs within each cell is studied at different scales. In particular, for each set of pixels with SCVs falling in a given cell q_m $(m = 1,2,\ldots,M)$ at full resolution, the behavior of the distribution of the same SCVs at resolution level $N-1$ (i.e., the lowest considered one) is analyzed in order to identify whether the cell is associated with registration noise or not. It is worth noting that the maximum level of decomposition $N-1$ has to be selected according to the size of expected main change structures in the considered images. The main idea of this procedure is to identify cells of registration noise through a comparison between the distribution of the magnitude of SCVs at full resolution and at the lowest considered resolution. At this level pixels of registration noise tend to disappear given their properties that usually result in small and thin structures. To this purpose, according to the multiscale properties described in the previous section, the behavior of the mean value of SCVs on the magnitude variable at different resolutions is analyzed. In the proposed method the mean value μ_{ρ,q_m}^0 of the magnitude ρ of SCVs that fall within a cell q_m at full resolution (level 0) is compared with the mean value μ_{ρ,q_m}^{N-1} that the same SCVs have at resolution level $N-1$.[2] A cell is associated with registration noise (RN) or not $(RNfree)$ according to the following decision rule:

$$q_m \in \begin{cases} RNfree, & \text{if } \left\{\left|\mu_{\rho,q_m}^0 - \mu_{\rho,q_m}^{N-1}\right| < K\right\} \\ RN, & \text{if } \left\{\left|\mu_{\rho,q_m}^0 - \mu_{\rho,q_m}^{N-1}\right| \geq K\right\} \end{cases} \tag{7}$$

where K is a threshold value empirically set as equal to the difference between the mean value of all the SCVs falling in A_c at full resolution and the mean value of the corresponding SCVs at the lowest level, i.e.,

$$K = \left|\mu_{\rho,A_c}^0 - \mu_{\rho,A_c}^{N-1}\right|. \tag{8}$$

It is worth noting that small variations of the threshold value around the automatic retrieved one do not significantly affect the identification of registration noise clusters.

Let q_m^{RN} be a generic cell q_m associated with registration noise according to (7). A generic SCV z_{ij} is associated with registration noise if it falls within a cell q_m^{RN}, i.e.,

$$z_{ij} \in \begin{cases} RN, & \text{if } z_{ij} \in q_m^{RN} \\ RNfree, & \text{otherwise.} \end{cases} \tag{9}$$

In this way we locate the SCVs affected by registration noise in the polar domain.

As pointed out previously, an important aspect to be considered is the choice of the quantization cell size. Slightly different results can be obtained with different quantization characterized by cell sizes in different ranges of parameters $\Delta\rho$ and $\Delta\vartheta$. Therefore in the third step we adopt a strategy capable to take advantage of different cell sizes, in order to make the technique less affected from the choice of these parameters. First of all the *annulus of changed pixels* is divided L times into uniformly distributed quantization cells with different size $\Delta\rho_l \times \Delta\vartheta_l$, $(l = 1,\ldots,L)$.

Let us define the set $\boldsymbol{Q}$ of all the L considered quantizations as

$$\boldsymbol{Q} = \{Q_l | l = 1,\ldots,L\} \tag{10}$$

[2]It is worth noting that in order to identify cells of registration noise we do not analyze the behavior of SCVs that fall within the same cell at different resolution levels, but we consider SCVs that at the highest resolution fall within a cell and the same SCVs at the lowest considered level. This approach allows us to follow the low-pass effect of the decomposition filter, which causes a migration of SCVs toward the origin of the polar domain.

Q_l $(l = 1, \ldots, L)$ is the lth quantization made up of a set of cells with the same size

$$Q_l = \left\{ q_m^l \left| \bigcup_{m=1}^{M_l} q_m^l = A_c, q_m^l = \Delta\rho_l \times \Delta\vartheta_l \right. \right\} \tag{11}$$

where M_l indicates the number of cells that results from the quantization process, given $\Delta\rho_l$ and $\Delta\vartheta_l$.

For each quantization Q_l the previously described procedure is performed in order to obtain labels RN and $RNfree$ for each cell of each quantization Q_l $(l = 1, \ldots, L)$. Let Θ_{ij} be the set of L labels (one for each Q_l) associated to z_{ij} according to (9). Labels in Θ_{ij} can assume values in $\{RN, RNfree\}$. In order to determine if a spectral change vector z_{ij} is of registration noise or not, a majority voting rule is applied to Θ_{ij}. Therefore a spectral change vector z_{ij} is of registration noise if the most of the labels in Θ_{ij} is RN, i.e.,

$$z_{ij} \in \begin{cases} RN, & \text{if } mode(\Theta_{ij}) = RN \\ RNfree, & \text{if } mode(\Theta_{ij}) = RNfree \end{cases} \tag{12}$$

where $mode(.)$ is the mathematical operator that returns the element that occurs most often in a set of elements. In other words, a generic region of A_c covered by cells (one for each Q_l) that are mostly associated to registration noise according to (7) is defined as registration noise region, otherwise it is registration noise free. Actually, this procedure implicitly results in a quantization Q_A of the *annulus of changed pixels* made up of regions with different shapes and sizes. Each region is labeled as RN or $RNfree$. We refer to these regions as adaptive cells q_a $(a = 1, \ldots, M_a)$, and Q_A results defined as

$$Q_A = \left\{ q_a \left| \bigcup_{a=1}^{M_a} q_a = A_c \right. \right\}. \tag{13}$$

Let q_a^{RN} $(a = 1, \ldots, M_a)$ be a generic adaptive cell which includes contiguous SCVs in the magnitude-direction domain that have been associated to label RN according to (12). Taking into account this notation, the rule (12) can be rewritten as:

$$z_{ij} \in \begin{cases} RN, & \text{if } z_{ij} \in q_a^{RN} \\ RNfree, & \text{otherwise.} \end{cases} \tag{14}$$

B. Context-Sensitive Decision Strategy for the Generation of the Final Change-Detection Map

The retrieved information on each adaptive cell is used for properly driving the generation of the final change-detection map according to a context-sensitive parcel-based procedure. Parcels are defined as regions that adaptively characterize the local neighborhood of each pixel in the considered scene and are homogeneous in both temporal images [23], [28]. The adaptive nature of multitemporal parcels allows one to model complex objects in the investigated scene as well as borders of the changed areas and geometrical details. In order to generate multitemporal parcels from the two original images we first compute two segmentation maps $P(\mathbf{X}_1)$ and $P(\mathbf{X}_2)$ applying a segmentation algorithm separately to images $\mathbf{X}_1$ and $\mathbf{X}_2$, respectively. In this work a region growing segmentation algorithm was considered, however any different kind of technique can be adopted. Each $P(\mathbf{X}_t)$ represents a partition of image $\mathbf{X}_t$ $(t = 1,2)$ in disjoint regions of spatially contiguous pixels. Each single region in both partitions satisfies a homogeneity measure $H(.)$ that involves spectral and spatial properties [31], [32]. The desired representation of the spatio-temporal context of the considered scene is obtained merging the two segmentations. The final output is a partition $P(\mathbf{X}_1, \mathbf{X}_2)$ shared by both considered images made of N regions p_r $(r = 1, \ldots, R)$ called parcels. The defined multitemporal parcels satisfy the following conditions:

$$\begin{aligned} &H\left[\mathbf{X}_1(p_r)\right] = true \quad \text{AND} \quad H\left[\mathbf{X}_2(p_r)\right] = true \\ &H\left[\mathbf{X}_1(p_r) \cup \mathbf{X}_1(p_k)\right] = false \quad \text{OR} \\ &\quad H\left[\mathbf{X}_2(p_r) \cup \mathbf{X}_2(p_k)\right] = false \\ &\quad \forall \quad r, k = 1, \ldots, R \quad \text{and} \quad r \neq k \end{aligned} \tag{15}$$

where $\mathbf{X}_t(p_r)$ represent the portion of image $\mathbf{X}_t$ $(t = 1,2)$ covered by parcel p_r $(r = 1, \ldots, R)$ and p_r and p_k are adjacent.

The spatial-context information associated to each parcel is integrated to the information about presence or absence of registration noise retrieved from the multiscale analysis in the previous phase. Let Z_r be the set of spectral change vectors corresponding to the pixels included in parcel p_r, i.e., $Z_r = \{z_{ij} | z_{ij} \in p_r\}$. Each SCV in Z_r can assume one out of three labels. Therefore the SCVs (i.e., the pixels) in a generic parcel p_r can be divided into three subsets: 1) Z_r^{RN} which includes SCVs of registration noise labeled according to (14); 2) Z_r^{RNfree} which includes SCVs that are not affected by registration noise according to (14); and 3) $Z_r^{\omega_n}$ which includes SCVs that fall into C_n. According to this notation, all the SCVs in a generic parcel p_r (and, thus, the parcel itself) are classified as changed or no-changed according to the following majority rule:

$$p_r \in \begin{cases} \omega_n, & \text{if } \frac{\left|Z_r^{RN}\right| + \left|Z_r^{\omega_n}\right|}{|Z_r|} \geq 0.5 \\ \Omega_c, & \text{otherwise} \end{cases} \tag{16}$$

where $|.|$ is the mathematical operator that returns the cardinality of sets. In other words a parcel p_r (and therefore all the pixels in it) is labeled as no-changed if the most of the SCVs belonging to it either have been classified as SCVs affected by registration noise according to (14) or fall into C_n. It is worth noting that the proposed approach allows us to create a relationship between the RN information retrieved in the polar domain (related to spectral change vectors) and the spatial information of the original images (related to pixels and parcels). The final change-detection map is obtained at full resolution, as low resolution components extracted from the multiscale analysis are used only for detecting quantization cells associated with registration noise. Thus, the obtained change-detection map adequately models geometrical details present in the analyzed VHR images, reproducing accurately both border and homogeneous changed regions.

IV. Experimental Results

In this section the experimental analysis conducted on real data is presented. First of all the data sets are described, then the multiscale properties presented in Section II-B are analyzed on the considered data. Finally the proposed multiscale and parcel-

based technique is applied to the images and results are discussed.

A. Data Set Description

In order to assess the effectiveness of the proposed technique, two multitemporal data sets were considered. In particular, two different portions of two images acquired on the city of Trento (Italy) by the QuickBird multispectral sensor in October 2005 and July 2006 were analyzed. The QuickBird sensor collects panchromatic images at 0.7 [m] resolution and multispectral images with four spectral channels (blue (450–520[nm]), green (520–600[nm]), red (630–690[nm]) and near-IR (760–900[nm])) at 2.8 [m] resolution. In the preprocessing phase the two images were: 1) pan-sharpened; 2) radiometrically corrected; and 3) coregistered. In particular, we considered pan-sharpened images as we expect that the pan-sharpening process can improve the results of the change-detection process, as demonstrated in previous work [29]. To this purpose we applied to the images the Gram–Schmidt procedure implemented in the ENVI software package [30] to the panchromatic channel and the four bands of the multispectral images. Concerning radiometric corrections, we simply normalized the images by subtracting from each spectral channel of the two considered images its mean value.

The two different data sets were selected with the following rationale: 1) the first data set (Data Set 1), which is made up of images of 984 $\times$ 984 pixels, is a small portion of the investigated scene for which we have a complete and detailed knowledge of the changes occurred on the ground. This allowed us to perform a quantitative detailed analysis under completely controlled conditions; 2) the second data set (Data Set 2), which is made up of images of 5000 $\times$ 5000 pixels, is related to the largest portions of the two available QuickBird images that correspond to the same area on the ground. These large images allowed us to perform a less detailed quantitative analysis (based upon a spatial random sampling as we did not have a complete knowledge of the changes occurred on the ground) but an important qualitative analysis on the effectiveness and robustness of the proposed technique in real operational conditions on large scenes. The registration process was carried out by using a polynomial function of order 2 according to 14 ground control points (GCPs) for the first data set and according to 20 GCPs for the second one, and by applying a nearest neighbor interpolation [30]. In our experiments we did not use more advanced registration techniques and procedures for geometric corrections for better assessing the robustness of the proposed method to the residual registration noise.

Fig. 6(a) and (b) the pansharpened images $\mathbf{X}_1$ and $\mathbf{X}_2$, respectively, related to the Data Set 1 (984 $\times$ 984 pixels). Between the two acquisitions two kinds of changes occurred: 1) simulated changes that consist of new houses introduced on the rural area [continuous circles in Fig. 6(b)]; and 2) real changes that consist of some roofs rebuilt in the urban area [dashed circles in Fig. 6(b)]. It is worth noting that simulated changes have been introduced in a completely realistic way in order to include a second type of change in the analysis. In particular, simulated buildings have been added to the scene taking their geometrical structures and spectral signatures from other real buildings present in other portions of the available full scene in order to take into account the image dynamic and noise properties. Moreover, between the two dates other spectral changes that depend upon differences in the vegetation phenology and have not a semantic meaning are present, due to the different acquisition seasons (i.e., summer and autumn) of the images under investigation. To perform a quantitative assessment of the effectiveness of the proposed method, a reference map (which includes 20602 changed pixels and 968256 no-changed pixels) was defined according to both the available prior knowledge on the considered area and to a visual analysis of images [see Fig. 6(c)]. According to the previous observation, the reference map does not report changes due to seasonal variations of the vegetation phenology. However, if these changes show significant intesity in the magnitude domain, they will appear in the final change-detection map, even if, from a semantic point of view, the related area is not changed.

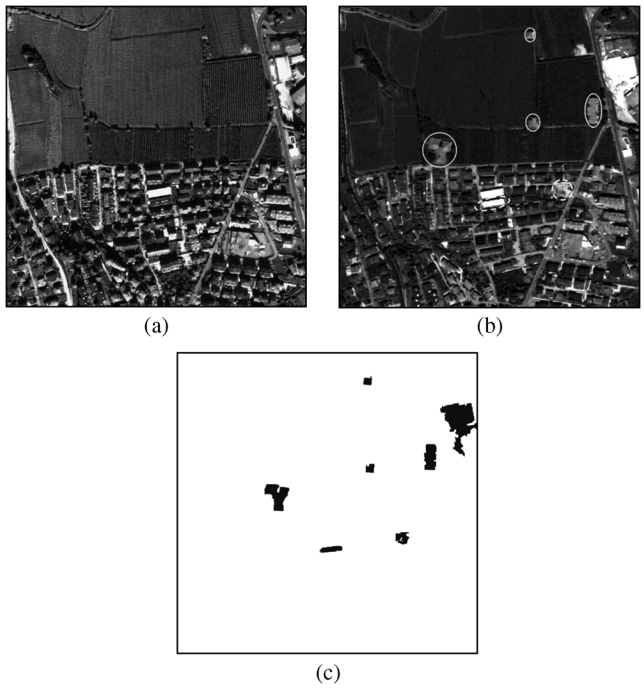

Fig. 6. Data Set 1 (small images) made up of pansharpened images of the Trento city (Italy) acquired by the QuickBird VHR multispectral sensor in: (a) October 2005; and (b) July 2006 (simulated changes appear in the regions marked with continuous circle, while real changes occurred between the two acquisition dates appear in regions marked with dashed circles). (c) Change-detection reference map.

Fig. 7(a) and (b) shows the pansharpened images $\mathbf{X}_1$ and $\mathbf{X}_2$, respectively, related to the Data Set 2 (5000 $\times$ 5000 pixels). Between the two acquisitions different kinds of changes occurred on the ground affecting urban, industrial, rural and forest areas. From a visual analysis it is possible to note: 1) differences in some roofs of the urban and industrial areas; 2) differences in the bank of the river due to a reduction of the water level; 3) significant differences due to shadows in the forest area; and 4) differences in the cultivated fields due to different kinds of farming. Considering the extent of the scene and the fact that we have no a priori information on the whole area under investigation, in this case it was not possible to derive a complete reference map. The

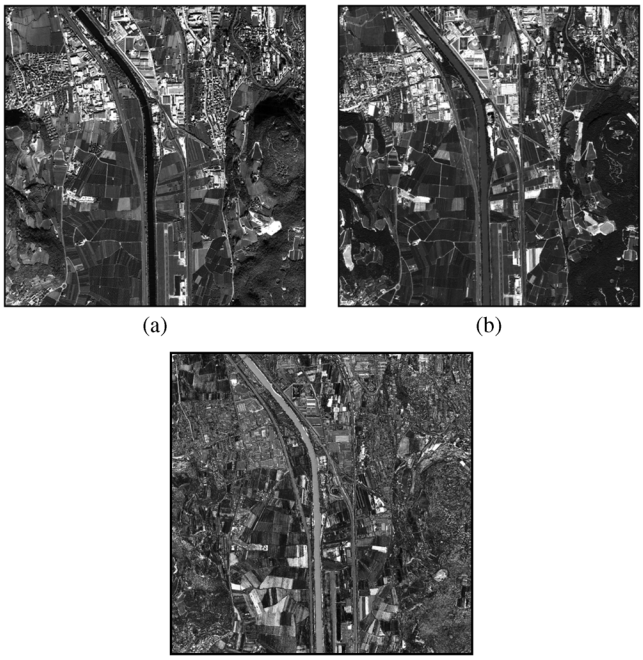

Fig. 7. Data Set 2 (large images) made up of pansharpened images of the Trento city (Italy) acquired by the QuickBird VHR multispectral sensor in: (a) October 2005 and (b) July 2006; (c) magnitude image.

magnitude image obtained according to (2) points out the main spectral differences present between the two dates [Fig. 7(c)]. To perform a quantitative assessment of the effectiveness of the proposed method on this large images, a set of points were randomly collected in the scene and each of them was labeled as changed or nonchanged according to a careful visual analysis. In particular, 2300 points were collected (245 labeled as change and 2055 as no-change). It is worth noting that in this case there are some semantic changes in the crops (i.e., changes in the type of cultivation), which are considered as changes in the reference map and, thus, in the quantitative analysis. Finally, also in this second data set changes related to different phenology of the vegetation are considered as false alarms, since they have not any semantic meaning.

B. Results: Multiscale Properties

To confirm the validity of the fundaments of the proposed technique, we carried out an analysis on the multiscale properties of registration noise on the considered images. This analysis was conducted only on Data Set 1, as a complete reference map on the investigated area was available only for the small images. The aim of this analysis was to show that the properties derived on simulated data are effective also for real data. To this purpose, as done for simulated data in [25] and reported in this work in Section II-B, from the QuickBird multitemporal images $\mathbf{X}_1$ and $\mathbf{X}_2$ we generated images at different scales by applying the *Daubechies*-4 stationary wavelet transform [26] to the multitemporal images $\mathbf{X}_1$ and $\mathbf{X}_2$. To show the effect of the multiscale decomposition in the polar domain, we applied the CVA technique to the original images and to the dataset

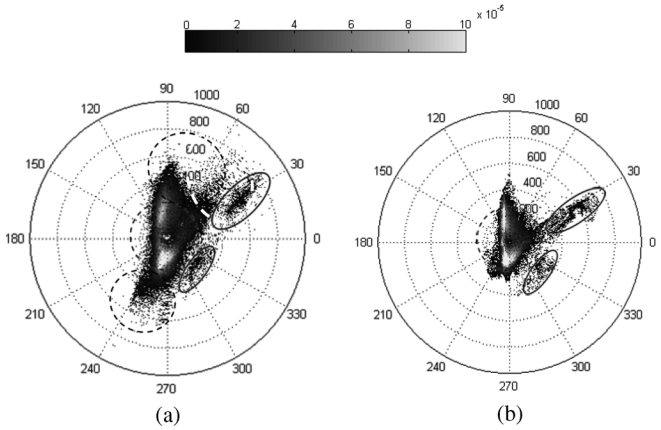

Fig. 8. Scatterograms in the polar coordinate system of (a) the full resolution original difference image, and (b) the low resolution image obtained at level four of the wavelet decomposition. Dotted circle separates C_n from A_c, continuous circles indicate sectors of true changes, while dashed circles identify regions of registration noise.

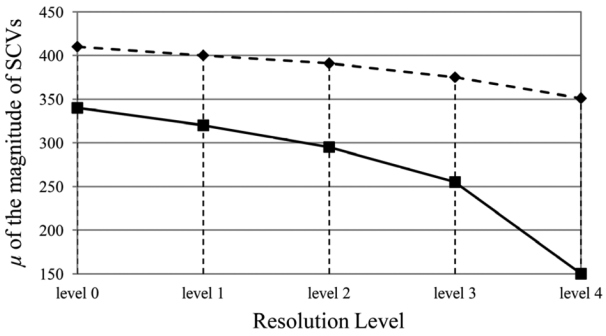

Fig. 9. Behavior of the mean value of the magnitude of SCVs versus the resolution levels (scale) for the class of changes (dashed line) and of registration noise (continuous line).

at lowest resolution. We considered only the red and near infrared spectral channels, as they revealed to be the most effective in emphasizing the changes occurred on the area of interest. Fig. 8 reports the scatterograms obtained on both the images at full resolution and the images at the fourth level of the decomposition. Comparing these scatterograms (and the other ones obtained at different resolution level, which are not reported for space constraints) it is possible to observe that, decreasing the resolution, clusters associated with changed pixels (see regions marked with continuous circles in Fig. 8) only reduce their spread, without being completely smoothed out. On the contrary, clusters associated with RN tend to disappear [dashed circles in Fig. 8(a)], collapsing within the *circle of no-changed pixels* [dotted circle in Fig. 8(a)]. This behavior confirms what expected from the analysis presented in Section II-B, i.e., SCVs of real changes show a quite stable trend, while SCVs associated with registration noise have non stable properties versus the scale. These results were conducted also on other data sets.

In greater detail, we studied the behavior of the mean values in the magnitude domain of SCVs related to registration noise and to real changes, when the resolution of the images decreases. Fig. 9 reports the behavior of the mean value of the magnitude of SCVs versus the scale: the mean value of RN clusters rapidly decreases by reducing the scale (continuous line), while the mean

value of SCVs associated with true changes slightly varies with the scale (dashed line), decreasing slower than the one of SCVs related to RN.

C. Results: Change Detection on Data Set 1 (Small Images)

The effectiveness of the proposed technique was first tested on the Data set 1. To this purpose cells of registration noise were identified according to the procedure described in Section III-A, and then the final change-detection map was generated according to Section III-B. According to the proposed technique, the first step aimed at identifying registration noise. To this purpose the change vector analysis technique was applied to images $\mathbf{X}_1$ and $\mathbf{X}_2$ and the decision threshold T that separates the *annulus of changed pixels* from the *circle of no-changed pixels* was computed. The Bayes rule for minimum error [17], [27] with estimates obtained by the Expectation Maximization (EM) algorithm was used for retrieving a value T equal to 220. SCVs in C_n were labeled as no-changed SCVs. Five $(L = 5)$ different quantizations Q_l $(l = 1, \ldots, 5)$ were considered for the *annulus of changed pixels* with cells of size $\Delta\rho_l \times \Delta\vartheta_l$, where $\Delta\rho_l \in \{100, 200, 300, 400, 500\}$ and $\Delta\vartheta_l = 10^\circ$ (for each $l = 1, \ldots, 5$). It is worth noting that different values for $\Delta\rho_l$ and $\Delta\vartheta_l$ can be selected according to the considered data set. Images $\mathbf{X}_1$ and $\mathbf{X}_2$ were decomposed according to the procedure described in Section IV-B, and the CVA technique was applied to the full (i.e., level 0) and the lowest (i.e., level four of the wavelet transform) resolution images. Fig. 8 shows the polar scatterograms obtained for the two mentioned resolution levels.

In order to identify whether a cell q_m^l $(l = 1, \ldots, M_l)$ for a given Q_l $(l = 1, \ldots, 5)$ is of registration noise or not the difference in the mean values of the magnitude of SCVs between the resolution level 0 and 4 was computed. This value was compared with the threshold K derived according to (8) (for T equal to 220, the value of K resulted equal to 190). SCVs falling into cells in which the difference resulted to be higher than K were labeled as belonging to registration noise according to (9). At this stage, for comparison purposes, a set of five change-detection maps was generated (one for each considered quantization) by assigning SCVs in C_n and SCVs of registration noise to the class of no-changed pixels and all the others to the class of changed pixels (see Table I). As one can see, for $\Delta\rho_l$ between 200 and 400 similar results were achieved, whereas higher or lower values resulted in slightly worse performance.

In order to reduce the impact of critical values of $\Delta\rho_l$ and $\Delta\vartheta_l$ on the change-detection performance, we applied the proposed technique for adaptively modeling the cell shape and size involving in the decision step all the five quantization intervals. Each SCV was classified as belonging to registration noise or not according to (12). Even at this stage, for sake of comparison, a change-detection map was computed by assigning SCVs in C_n and SCVs of registration noise to the class of no-changed pixels and all the others to the class of changed pixels (see results for the pixel-based proposed technique in Table II). Comparing these results with the ones in Table I it is possible to conclude that the joint use of quantization cells of different size makes the change-detection process more robust as results obtained with unreliable quantizations values are discarded thanks to the majority decision rule in (12).

TABLE I
CHANGE-DETECTION RESULTS OBTAINED ON DATA SET 1 (SMALL IMAGES) AT A PIXEL LEVEL WITH THE PROPOSED MULTISCALE TECHNIQUE WITHOUT THE ADAPTIVE ANALYSIS OF THE CELL DIMENSION

Cell size $(\Delta\rho_l \times \Delta\vartheta_l)$	False alarms	Missed alarms	Overall error	Overall accuracy (%)
100x10	111279	17356	128635	86.72
200x10	61252	5123	66375	93.15
300x10	62867	4728	67595	93.02
400x10	63091	4644	67735	93.00
500x10	76614	17905	94519	90.24

TABLE II
CHANGE-DETECTION RESULTS OBTAINED ON DATA SET 1 (SMALL IMAGES) AT BOTH PIXEL AND PARCEL LEVEL BY THE PROPOSED ADAPTIVE AND MULTISCALE TECHNIQUE, THE STANDARD CVA TECHNIQUE AND THE MANUAL APPROACH

	Technique	False alarms	Missed alarms	Overal l error	Overall accuracy (%)
Pixel-based	**Proposed**	61429	5061	66490	93.13
	Standard CVA	173676	1470	175146	81.91
	Manual (upperbound)	55984	5768	61752	93.62
Parcel-based	**Proposed**	28150	3870	32020	96.69
	Standard CVA	106580	734	107314	88.92
	Manual (upperbound)	23160	4192	27352	97.18

Finally, the information about adaptive cells of registration noise was used within the parcel-based decision strategy for computing the final change-detection map according to the proposed strategy. To this end, multitemporal parcels were generated as described in Section III-B and SCVs in each parcel were labeled according to (16). As one can see from Table II, the use of the spatial-context information significantly reduces both false and missed alarms. It is worth noting that the use of spatial-context information retrieved according to the parcel-based strategy allows one to obtain a regularized change-detection map without affecting the geometrical details content of the map itself.

For a further assessment of the effectiveness of the proposed technique, change detection was performed according to the standard pixel-based [17] and parcel-based [28] change vector analysis ignoring the information about registration noise. In both cases (see Table II) it is clear that standard methods are sharply affected by the presence of registration noise, which involves a high number of false alarms mainly located in the high frequency regions of the images. On the contrary, the proposed method significantly reduces false alarms both at pixel (from 17.94% to 6.34%) and at parcel level (from 11.01% to 2.91%), and generates change-detection maps characterized by high accuracy both in homogeneous and border areas. Fig. 10 allows

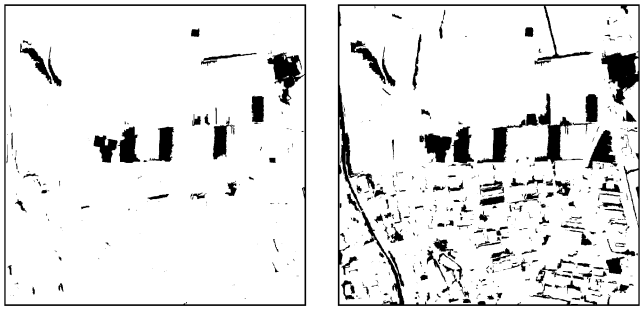

(a) (b)

Fig. 10. Change-detection maps obtained on Data Set 1 with: (a) proposed multiscale approach with the adaptive estimation of the cell dimension at a parcel level; and (b) the standard parcel-based CVA.

TABLE III
CHANGE-DETECTION RESULTS OBTAINED ON DATA SET 2 (LARGE IMAGES) AT BOTH PIXEL AND PARCEL LEVEL BY THE PROPOSED ADAPTIVE AND MULTISCALE TECHNIQUE AND THE STANDARD CVA TECHNIQUE

	Technique	False alarms	Missed alarms	Overall error	Overall accuracy (%)
Pixel-based	Proposed	74	51	125	94.56
	Standard CVA	274	23	297	87.07
Parcel-based	Proposed	21	41	62	97.10
	Standard CVA	160	41	201	91.25

one a visual comparison between the change-detection map obtained at parcel level with the proposed technique [Fig. 10(a)] and the standard CVA [Fig. 10(b)].

A final comparison is made with the results achieved according to a manual trial-and-error approach. In this case the final change-detection map is computed assigning SCVs that fall into C_n to ω_n, and applying manual thresholds for isolating within A_c SCVs associated with changed pixels from those associated with registration noise on the basis of some prior information. Two maps were generated. The first considers the spatial-context information arising from multitemporal parcels while the second does not. Results yielded with this procedure can be considered as an upper bound for the proposed technique. Observing Table II, one can conclude that the proposed method performs effectively both at a pixel and at a parcel level, as it exhibits overall accuracies that are close to those obtained by the manual (optimal) approach (i.e., 93.13% vs. 93.62% for the pixel-based case and 96.69% vs. 97.18% for the parcel-based one).

As final remark it is important to notice that the change-detection map derived by the proposed approach presents residual false alarms mainly due to the different acquisition seasons of the considered images (i.e., summer and autumn). This characteristic resulted in significant radiometric differences related to seasonal variations in the crop rows and in the shapes of shadows. The false alarms due to such acquisition conditions can be reduced only considering additional semantic information associated with changes. However, the overall accuracy achieved by the proposed context-sensitive technique robust to registration noise (i.e., 96.69%) due to sharp reduction of false alarms and the high fidelity in the reproduction of changed objects (both in uniform and contour regions) confirms its validity.

D. Results: Change Detection on Data Set 2 (Large Images)

In order to study the effectiveness of the proposed method in real operational conditions (where large images are considered), this sub-section reports the results obtained on the Data Set 2. As described for the previous data set, cells of registration noise were identified and then the final change-detection map was generated. In order to identify registration noise, we decomposed the images through the *Daubechies*-4 stationary wavelet transform and we applied the CVA technique to the images $\mathbf{X}_1$ and $\mathbf{X}_2$ at full resolution and at the lowest considered level (fourth level of the wavelet transform). Also in this case the threshold value T ($T = 320$) that separated A_c from C_n was retrieved according to the Bayes rule for minimum error. Five different quantization Q_l ($l = 1, \ldots, 5$) of the *annulus of changed pixels* with cells of size $\Delta\rho_l \times \Delta\vartheta_l$, where $\Delta\rho_l \in \{100, 200, 300, 400, 500\}$ and $\Delta\vartheta_l = 5°$ (for each $l = 1, \ldots, 5$), were considered. Then the analysis on the difference in the mean values of the SCVs that fall within each cell at full resolution and at low resolution was performed and compared with the threshold K derived according to (8) ($K = 98$), in order to label each SCVs as belonging to RN or not according to (9). At this point the proposed technique for adaptively modeling the cell shape was applied to the five different considered quantizations Q_l and the final change-detection map at a pixel level was generated by assigning SCVs in C_n and SCVs of registration noise to the class of no-changed pixels and the others to the class of changes pixels (see results in Table III).

Finally, the contextual information was exploited through the parcel-based proposed strategy and the final change-detection map at a parcel level was generated. Numerical results obtained on the test set described in Section IV-A are reported in Table III. As one can observe, also in this case the number of false alarms is significantly reduced in the parcel-based strategy.

As for the Data Set 1, we compared the results obtained with the proposed method with the ones achieved by the standard CVA both at pixel and parcel level ignoring the information about registration noise. Observing Table III, it is clear that in both cases the standard method is sharply affected by a high number of false alarms (mainly due to RN), whereas the proposed method exhibits a significant reduction of them, resulting in an overall change detection accuracy 6% higher than that achieved by the standard method (from 87.07% to 94.56% for the pixel-based case and from 91.25% to 97.10% for the parcel-based case).

Fig. 11(a) and (b) report the change-detection maps obtained at a parcel level with the proposed method and with the standard CVA, respectively. A visual analysis of them confirms the effectiveness of the parcel-based method in representing correctly both homogeneous and border regions, and shows the sharp reduction of false alarms due to RN with the proposed method, especially in the urban area of the considered scene (upper left part of the image).

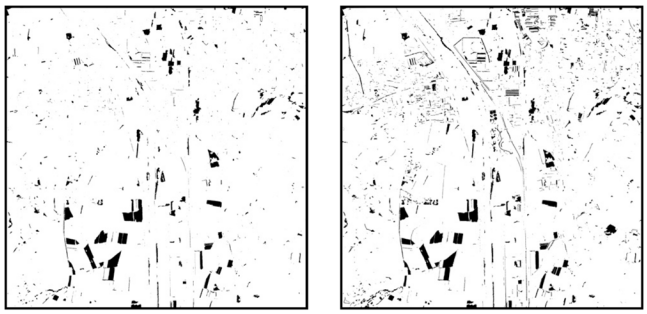

(a) (b)

Fig. 11. Change-detection map obtained on Data Set 2 with: (a) proposed multiscale approach with adaptive estimation of the cell dimension at parcel level; and (b) the standard parcel-based CVA. (It is worth noting that the maps represent an area of 5000 × 5000 pixels and, thus, many changes are not clearly visible).

Results obtained on the large data set are very similar to the ones obtained on the small one. This proves the effectiveness of the proposed method also on large images which are a typical condition in real operational applications.

V. Conclusion

In this paper we presented a context-sensitive multiscale technique robust to registration noise for change detection on very high geometrical resolution multispectral images.

When dealing with change detection in multitemporal VHR images one of the most significant sources of errors is registration noise. Such kind of noise is due to the impossibility to perfectly align multitemporal images even if accurate co-registration techniques are applied to the data. In order to understand how to reduce the impact of residual misregistration on the change-detection process, in this work we carried out an analysis of the behaviors of registration noise that affect multitemporal VHR data sets. This analysis was developed in the context of a polar framework for change vector analysis. It was observed that SCVs that fall into the annulus of changed pixels but are associated with registration noise (and therefore are a possible source of false alarms) exhibit significant variations of statistical properties as the scale is reduced. According to this observation, the proposed approach performs a quantization-based multiscale analysis of SCVs in the magnitude-direction domain in order to identify SCVs associated with registration noise. The retrieved information on registration noise is then exploited in the framework of a parcel-based decision strategy that takes advantage of spatial-context information in defining the final change-detection map. This step is performed at full resolution in order to preserve all the high geometrical detail information characteristic of VHR images.

The qualitative and quantitative analysis of the results obtained on two data sets made up of a small and a large pair of QuickBird images point out that the proposed technique involves a low amount of false alarms in change-detection maps and a high accuracy in modeling both geometrical details and homogeneous areas. In greater detail, the achieved results are significantly better than the ones yielded by standard change-detection techniques. The effectiveness of the proposed technique was also tested on different data sets acquired by different remote sensing sensors (that are not reported for space constraint), which confirmed the conclusion drawn for the presented QuickBird data.

Symbol	Description	Symbol	Description
$\mathbf{X}_t$	VHR multispectral image acquired at time t	RN	Label of SCVs associated with registration noise
Ω	Set of the considered information classes	$RNfree$	Label of SCVs non associated with registration noise
ω_n	Class of no-changed pixels	K	Threshold that separate RN from $RNfree$ SCVs
Ω_c	Set of classes of change	q_m^{RN}	mth cell associated with registration noise
ω_{ck}	Class of kth kind of change	L	Number of considered quantization steps
$\mathbf{X}_D$	Multispectral difference image	$\mathcal{Q}$	Set of L considered quantization steps
ϑ	Direction variable in the polar domain	$\mathcal{Q}_l$	Set of cells of for the lth quantization step
ρ	Magnitude variable in the polar domain	M_l	Number of quantization cells in $\mathcal{Q}_l$
$X_{b,D}$	bth component of $\mathbf{X}_D$	q_m^l	mth quantization cell in $\mathcal{Q}_l$
MD	Magnitude-Direction domain	$\Delta\vartheta_l$	q_m^l extension along direction
ρ_{max}	Highest value of the magnitude of SCVs in $\mathbf{X}_D$	$\Delta\rho_l$	q_m^l extension along magnitude
z_{ij}	SCV corresponding to spatial position (i,j)	Θ_{ij}	Set of L labels $\{RN, RNfree\}$ associated to z_{ij}
ϑ_{ij}	Direction of z_{ij}	$\mathcal{Q}_A$	Set of adaptive quantization cells in A_c
ρ_{ij}	Magnitude of z_{ij}	q_a	ath adaptive quantization cell in $\mathcal{Q}_A$
C_n	Circle of no-changed pixels	q_a^{RN}	Adaptive cell associated with registration noise
A_c	Annulus of changed pixels	M_a	Number of adaptive cells
T	Magnitude threshold that separates C_n from A_c	$H(.)$	Homogeneity measure for segmentation
S_k	Annular sector of change $\omega_{c_k} \in \Omega_c$	$P(\mathbf{X}_t)$	Partition of $\mathbf{X}_t$ in disjoint regions
$\vartheta_{k_1}, \vartheta_{k_2}$	Direction thresholds that bounds S_k	$P(\mathbf{X}_1,\mathbf{X}_2)$	partition shared by $\mathbf{X}_1$ and $\mathbf{X}_2$ (parcel)
$\mathbf{X}_{MS_t}$	Set of multiscale images obtained from $\mathbf{X}_t$	R	Number of disjoint parcels in $P(\mathbf{X}_1,\mathbf{X}_2)$
$\mathbf{X}_t^n$	Image at scale n in $\mathbf{X}_{MS_t}$	p_r	rth parcel in $P(\mathbf{X}_1,\mathbf{X}_2)$
N	Number of considered resolution levels	$\mathbf{X}_t(p_r)$	Portion of $\mathbf{X}_t$ covered by p_r
q_m	mth quantization cell	Z_r	Set of SCVs in p_r
M	Total number of quantization cells q_m	Z_r^{RN}	Set of SCVs of registration noise in p_r
$\Delta\vartheta$	q_m extension along direction variable	Z_r^{RNfree}	Set of registration noise free SCVs in p_r
$\Delta\rho$	q_m extension along magnitude variable	$Z_r^{\omega_n}$	Set of no-changed SCVs in p_r
μ^0_{ρ,q_m}	Mean value of the magnitude of SCVs that fall in q_m at full resolution	μ^0_{ρ,A_c}	Mean value of the magnitude of SCVs that fall in A_c at full
μ^{N-1}_{ρ,q_m}	Mean value of the magnitude of SCVs, that fall in q_m at level 0, at resolution N-1	μ^{N-1}_{ρ,A_c}	Mean value of the magnitude of SCVs, that fall in A_c at level 0, at resolution N-1

An additional remark concerns the residual false alarms present in the final change-detection map yielded by the proposed technique. These errors are mainly related to radiometric changes induced by seasonal variations which are not relevant to the considered application. Although we did not consider this aspect in this work, such false alarms can be reduced only considering additional semantic information about the kind of changes present on the ground.

It is worth noting that despite the proposed method was developed for VHR remote sensing images (as the impact of misregistration on this kind of data is more relevant), it can be suitable also for the analysis of optical data at lower resolution and, under given conditions, also for other kinds of images.

As a future work we plan to extensively test the proposed method on other multitemporal images acquired by different sensors representing different change-detection problems.

APPENDIX I

Please see the chart on the previous page.

REFERENCES

[1] L. H. Chen and S. Chang, "A video tracking system with adaptive predictors," *Pattern Recognit.*, vol. 25, no. 10, pp. 1171–1180, 1992.

[2] W. Y. Kan, J. V. Krogmeier, and P. C. Doerschuk, "Model-based vehicle tracking from image sequences with an application to road surveillance," *Opt. Eng.*, vol. 35, no. 6, pp. 1723–1729, 1996.

[3] L. Li, W. Huang, I. Y.-H. Gu, and Q. Tian, "Statistical modeling of complex backgrounds for foreground object detection," *IEEE Trans. Image Process.*, vol. 13, no. 11, pp. 1459–1472, Nov. 2004.

[4] S. C. Liu, C. W. Fu, and S. Chang, "Statistical change detection with moments under time-varying illumination," *IEEE Trans. Image Process.*, vol. 7, no. 9, pp. 1258–1268, Sep. 1998.

[5] C. Dumontier, F. Luthon, and J.-P. Charras, "Real-time DSP implementation for MRF-based video motion detection," *IEEE Trans. Image Process.*, vol. 8, no. 10, pp. 1341–1347, Oct. 1999.

[6] L. Li and M. K. H. Leung, "Integrating intensity and texture differences for robust change detection," *IEEE Trans. Image Process.*, vol. 11, no. 2, pp. 105–112, Feb. 2002.

[7] L. Bruzzone and S. B. Serpico, "An iterative technique for the detection of land-cover transitions in multitemporal remote-sensing images," *IEEE Trans. Geosci. Remote Sens.*, vol. 35, no. 4, pp. 858–867, Jul. 1997.

[8] L. Bruzzone and S. B. Serpico, "Detection of changes in remotely sensed images by the selective use of multi-spectral information," *Int. J. Remote Sens.*, vol. 18, no. 18, pp. 3883–3888, 1997.

[9] M. Bosc, F. Heitz, J. P. Armspach, I. Namer, D. Gounot, and L. Rumbach, "Automatic change detection in multimodal serial MRI: Application to multiple sclerosis lesion evolution," *Neuroimage*, vol. 20, pp. 643–656, 2003.

[10] M. J. Dumskyj, S. J. Aldington, C. J. Dore, and E. M. Kohner, "The accurate assessment of changes in retinal vessel diameter using multiple frame electrocardiograph synchronised fundus photography," *Current Eye Res.*, vol. 15, no. 6, pp. 652–632, Jun. 1996.

[11] A. Singh, "Digital change detection techniques using remotely-sensed data," *Int. J. Remote Sens.*, vol. 10, no. 6, pp. 989–1003, 1989.

[12] R. J. Radke, S. Andra, O. Al-Kofahi, and B. Roysam, "Image change detection algorithms: A systematic survey," *IEEE Trans. Image Process.*, vol. 14, no. 3, pp. 294–307, Mar. 2005.

[13] P. R. Coppin, I. Jonckheere, and K. Nachaerts, "Digital change detection in ecosystem monitoring: A review," *Int. J. Remote Sens.*, vol. 25, no. 9, pp. 1565–1596, May 2004.

[14] D. Lu, P. Mausel, E. Brondízio, and E. Moran, "Change detection techniques," *Int. J. Remote Sens.*, vol. 25, no. 12, pp. 2365–2407, Jun. 2004.

[15] M. J. Carlotto, "Detection and analysis of change in remotely sensed imagery with application to wide area surveillance," *IEEE Trans. Image Process.*, vol. 6, no. 1, pp. 189–202, Jan. 1997.

[16] F. Bovolo and L. Bruzzone, "A theoretical framework for unsupervised change detection based on change vector analysis in polar domain," *IEEE Trans. Geosci. Remote Sens.*, vol. 45, no. 1, pp. 218–236, Jan. 2007.

[17] L. Bruzzone and D. F. Prieto, "Automatic analysis of the difference image for unsupervised change detection," *IEEE Trans. Geosci. Remote Sens.*, vol. 38, no. 3, pp. 1171–1182, May 2000.

[18] J. R. G. Townshend, C. O. Justice, and C. Gurney, "The impact of misregistration on change detection," *IEEE Trans. Geosci. Remote Sens.*, vol. 30, no. 5, pp. 1054–1060, Sep. 1992.

[19] X. Dai and S. Khorram, "The effects of image misregistration on the accuracy of remotely sensed change detection," *IEEE Trans. Geosci. Remote Sens.*, vol. 36, no. 5, pt. 1, pp. 1566–1577, Sep. 1998.

[20] L. Bruzzone and R. Cossu, "An adaptive approach for reducing registration noise effects in unsupervised change detection," *IEEE Trans. Geosci. Remote Sens.*, vol. 41, no. 11, pp. 2455–2465, Nov. 2003.

[21] J. Li, S. Qian, and X. Chen, "Object-oriented method of land cover change detection approach using high spatial resolution remote sensing data," *IEEE Trans.Geosci. Remote Sens.*, vol. 5, pp. 3005–3007, 2003.

[22] F. Bovolo, L. Bruzzone, and S. Marchesi, "A multiscale change detection technique robust to registration noise," *Pattern Recognit. Mach. Intell.*, vol. 4815, pp. 77–86, 2007.

[23] F. Bovolo, "A multilevel parcel-based approach to change detection in very high resolution multitemporal images," *IEEE Geosci. Rem. Sens. Lett.*, vol. 6, no. 1, pp. 33–37, Jan. 2009.

[24] I. Niemeyer, P. R. Marpu, and S. Nussbaum, "Change detection using the object features," in *Proc. IEEE Int. Geoscience Remote Sense Symp.*, 2007, pp. 2374–2377.

[25] F. Bovolo, L. Bruzzone, and S. Marchesi, "Analysis and adaptive estimation of the registration noise distribution in multitemporal VHR images," *IEEE Trans. Geosci. Rem. Sens.*, vol. 47, no. 8, pt. 1, pp. 2658–2671, Aug. 2009.

[26] S. G. Mallat, "A theory for multiresolution signal decomposition: The wavelet representation," *IEEE Trans. Pattern Anal. Mach. Intell.*, vol. PAMI-11, no. 7, pp. 674–693, Jul. 1989.

[27] L. Bruzzone and D. F. Prieto, "An adaptive semiparametric and context-based approach to unsupervised change detection in multitemporal remote-sensing images," *IEEE Trans. Image Process.*, vol. 11, no. 4, pp. 452–466, Apr. 2002.

[28] L. Bruzzone and D. F. Prieto, "An adaptive parcel-based technique for unsupervised change detection," *Int. J. Remote Sens.*, vol. 21, no. 4, pp. 817–822, 2000.

[29] F. Bovolo, L. Bruzzone, L. Capobianco, A. Garzelli, S. Marchesi, and F. Nencini, "Change detection from pansharpened images: A comparative analysis," *IEEE Geosci. Remote Sens. Lett.*, vol. 7, no. 1, pp. 53–57, 2010.

[30] *"ENVI User Manual"* 2003 [Online]. Available: http://www.RSInc.com/envi, Boulder, CO: RSI

[31] M. Baatz, U. Benz, S. Dehghani, M. Heynen, A. Höltje, P. Hofmann, I. Lingenfelder, M. Mimler, M. Sohlbach, M. Weber, and G. Willhauck, *eCognition User Guide 4*. Parsippany, NJ: Definiens Imaging, 2004 [Online]. Available: http://www.definiens-imaging.com

[32] L. Bruzzone and L. Carlin, "A multilevel context-based system for classification of very high spatial resolution images," *IEEE Trans. Geosci. Remote Sens.*, vol. 44, no. 9, pp. 2587–2600, Sep. 2006.

Silvia Marchesi (S'08) received the laurea (B.S.) and laurea specialistica (M.S.) degrees in telecommunication engineering (summa cum laude) from the University of Trento, Italy, in 2005 and 2007, respectively, and is pursuing the Ph.D. degree in information and communication technologies at the same university.

She is currently with the Remote Sensing Group at the Department of Information Engineering and Computer Science, University of Trento. Her main research activity is in the area of remote-sensing image processing; in particular, her interests are related to change detection in very high geometrical resolution images.

Ms. Marchesi is a referee for the *IEEE Geoscience and Remote Sensing Letters*.

Francesca Bovolo (S'05–M'07) received the Laurea (B.S.) and the Laurea Specialistica (M.S.) degrees (*summa cum laude*) in telecommunication engineering and the Ph.D. degree in communication and information technologies from the University of Trento, Trento, Italy, in 2001, 2003, and 2006, respectively.

She is currently a Postdoctoral member with the Remote Sensing Laboratory, Department of Information Engineering and Computer Science, University of Trento. Her main research activity is in the area of remote-sensing image processing. In particular, her interests are related to multitemporal remote-sensing image analysis and change detection in multispectral and SAR images, and very high resolution images. She conducts research on these topics within the frameworks of several national and international projects.

Dr. Bovolo is a referee for the IEEE TRANSACTIONS ON GEOSCIENCE AND REMOTE SENSING; IEEE GEOSCIENCE AND REMOTE SENSING LETTERS; IEEE JOURNAL OF SELECTED TOPICS IN APPLIED EARTH OBSERVATIONS AND REMOTE SENSING; *International Journal of Remote Sensing*; *Pattern Recognition*; *Remote Sensing of Environment*; *Photogrammetric Engineering and Remote Sensing*; *Photogrammetry and Remote Sensing*; IEEE TRANSACTIONS ON AEROSPACE AND ELECTRONIC SYSTEMS; *Sensors*. She ranked first place in the Student Prize Paper Competition of the 2006 IEEE International Geoscience and Remote Sensing Symposium (Denver, August 2006). Since 2006, she has been with the Scientific Committee, SPIE International Conference on "Signal and Image Processing for Remote Sensing." She has served on the Scientific Committee of the IEEE Fourth and Fifth International Workshop on the Analysis of Multi-Temporal Remote Sensing Images (MultiTemp 2007 and 2009).

Lorenzo Bruzzone (S'95–M'98–SM'03–F'10) received the Laurea (M.S.) degree (*summa cum laude*) in electronic engineering and the Ph.D. degree in telecommunications from the University of Genoa, Genoa, Italy, in 1993 and 1998, respectively.

From 1998 to 2000, he was a Postdoctoral Researcher with the University of Genoa. Since 2000, he has been with the University of Trento, Trento, Italy, where he is currently a Full Professor of telecommunications. He teaches remote sensing, pattern recognition, radar, and electrical communications. He is the Head of the Remote Sensing Laboratory, Department of Information Engineering and Computer Science, University of Trento. He is an Evaluator of project proposals for many different governments (including the European Commission) and scientific organizations. He conducts and supervises research on these topics within the frameworks of several national and international projects. He is a Referee for many international journals and has served on the Scientific Committees of several international conferences. He is the author (or coauthor) of 74 scientific publications in referred international journals, more than 140 papers in conference proceedings, and seven book chapters. His current research interests are in the area of remote-sensing image processing and recognition (analysis of multitemporal data, feature extraction and selection, classification, regression and estimation, data fusion, and machine learning).

Dr. Bruzzone is a member of the Managing Committee of the Italian Inter-University Consortium on Telecommunications and a member of the Scientific Committee of the India–Italy Center for Advanced Research. He is also a member of the International Association for Pattern Recognition and of the Italian Association for Remote Sensing. Since 2009, he has been a member of the Administrative Committee of the IEEE Geoscience and Remote Sensing Society. He ranked first place in the Student Prize Paper Competition of the 1998 IEEE International Geoscience and Remote Sensing Symposium (Seattle, July 1998). He was a recipient of the Recognition of IEEE TRANSACTIONS ON GEOSCIENCE AND REMOTE SENSING Best Reviewers in 1999 and was a Guest Editor of a Special Issue of the IEEE TRANSACTIONS ON GEOSCIENCE AND REMOTE SENSING on the subject of the analysis of multitemporal remote-sensing images (November 2003). He was the General Chair and Cochair of the First and Second IEEE International Workshop on the Analysis of Multi-temporal Remote-Sensing Images (MultiTemp), and is currently a member of the Permanent Steering Committee of this series of workshops. Since 2003, he has been the Chair of the SPIE Conference on Image and Signal Processing for Remote Sensing. From 2004 to 2006, he served as an Associated Editor of the IEEE GEOSCIENCE AND REMOTE S LETTERS, and currently is an Associate Editor for the IEEE TRANSACTIONS ON GEOSCIENCE AND REMOTE SENSING.